Journal of Alloys and Compounds 508 (2010) 177–183

Contents lists available at ScienceDirect

Journal of Alloys and Compounds

journal homepage: www.elsevier.com/locate/jallcom

Elastic properties of Ni_2MnGa from first-principles calculations

S. Ozdemir Kart[a,*], T. Cagın[b]

[a] Department of Physics, Pamukkale University, Kınıklı Campus, 20017 Denizli, Turkey
[b] Department of Chemical Engineering, Texas A&M University, Texas, TX 77845-3122, USA

ARTICLE INFO

Article history:
Received 9 February 2010
Received in revised form 6 August 2010
Accepted 12 August 2010
Available online 19 August 2010

Keywords:
Magnetic shape memory alloy
Elastic constants
Debye temperature

ABSTRACT

Elastic properties of Ni_2MnGa in both austenitic and martensitic structures are determined by using *ab initio* methods based on density functional theory (DFT) within the spin-polarized generalized-gradient approximation. The tetragonal shear elastic constant C' takes a very small value in the austenitic phase, indicating the elastic instability results in a phase transition to martensitic structure. Isotropic mechanical properties such as bulk modulus, shear modulus, Young's modulus and Poisson's ratio are predicted. The trend of the Debye temperatures calculated for three structures of Ni_2MnGa is comparable with that of the experiment.

1. Introduction

Magnetic shape memory alloys (MSMAs) differ from traditional, thermally activated SMAs in that they are characterized by strong *magnetoelastic* coupling. The Heusler-type metals, such as Ni–Mn–X (X: Al, Ga, In, Sn, Sb), undergo martensitic transformations that are sensitive to alloy composition, external pressure, and applied magnetic field. Certain compositions display unique structural responses to external magnetic fields, undergoing either magnetic twin reorientation or field-induced phase transformations that lead to a macroscopic shape memory effect. In Ni–Mn–Ga, this effect generates recoverable strains that are an order-of-magnitude larger than those associated with the most common commercial magnetostrictors [1]. Since this discovery, Mn-based Heusler compounds have been heavily studied, both through experimental probing of structure-property relationships and theoretical modeling of the underlying mechanisms. Especially, Ni–Mn–Ga magnetic shape memory alloys serve as a reference system for all fundamental and applied studies related to magnetic shape memory (MSM) technology due to their unique magneto-mechanical properties. They can be used for development of sensors and actuators with rather high frequency compared to temperature driven conventional shape memory alloys and have larger shape changes than ordinary magnetostrictive materials. To be more specific, for instance Terfonel-D alloys exhibit magnetostrictive strains up to 0.17% [2]. In contrast, the structural deformation in Ni_2MnGa can reach about 10% under moderate magnetic fields on the order of 1 T [3].

MSM effect in Ni_2MnGa is caused by structural transformation from a higher symmetry cubic $L2_1$ (austenite) structure to a variety of different lower symmetry structures (martensite) upon cooling. Depending mostly on the composition, the martensitic structure is characterized by the tetragonal 5M modulated structure with $c/a \cong 0.94$, the orthorhombic 7M structure with $c/a \cong 0.9$, and the nonmodulated (NM) tetragonal structure with $c/a \cong 1.2$ [4]. The crystal structure of martensite is an important factor that determines the maximal magnetic field induced strain (MFIS) value described as $1 - c/a$. The structural deformation in the 5M modulated phase can reach 6% [5,6], while much larger (up to 10%) MFIS has been observed in 7M martensite [3]. However, NM tetragonal martensite does not exhibit any MSM behavior due to the appearance of high twinning stresses (approximately 6–18 MPa in this phase) [7].

Numerous studies aiming to understand the physical mechanism governing the martensitic phase transition have been performed in recent years. It has been reported that the stability of structural phases in Ni–Mn–Ga can be provided by the average change in both the valence electrons per atom (e/a) and tetragonality ratio (c/a) with composition as well as the martensitic transition temperature [8–14]. These studies suggest that, at low e/a (<7.7) the 5M phase exists, 7M structure is observed at the intermediate e/a, and the structure is tetragonal NM at high e/a (>7.7). Moreover, it has been estimated that the martensitic transition temperature increases with the e/a ratio. However, the effect of lattice dynamics on the lattice instability resulting in large MFIS has not yet been investigated enough [9]. Enkovaara et al. [15] predicted the phase transition temperature ($T_M \cong 175$ K) from austenite to martensite with $c/a = 1.27$ by calculating the vibrational free energy within the Debye approximation. More recently, Uijttewaal et al. [16] determined the free energies of the austenite, the modulated

* Corresponding author. Tel.: +90 258 2963587; fax: +90 258 2963535.
E-mail address: ozsev@pau.edu.tr (S. Ozdemir Kart).

0925-8388/$ – see front matter © 2010 Elsevier B.V. All rights reserved.
doi:10.1016/j.jallcom.2010.08.039

Table 1
Applied strains and corresponding strain energy densities for austenitic, NM and 5M martensitic structures. Unlisted compounds of strain are taken as zero for each case.

Phase	Strain	Parameters	$\Delta E/V_0$
Austenite	C1	$\varepsilon_1=\varepsilon_2=\varepsilon_3=\delta$	$\frac{3}{2}(C_{11}+2C_{12})\delta^2$
	C2	$\varepsilon_1=\delta, \varepsilon_2=-\delta, \varepsilon_3=\delta^2/(1-\delta^2)$	$(C_{11}-C_{12})\delta^2+O(\delta^4)$
	C3	$\varepsilon_3=\delta^2/(1-\delta^2), \varepsilon_6=\delta$	$2C_{44}\delta^2+O(\delta^4)$
Martensite NM	T1	$\varepsilon_1=\delta^2/(1-\delta^2), \varepsilon_4=\delta$	$2C_{44}\delta^2+O(\delta^4)$
	T2	$\varepsilon_3=\delta^2/(1-\delta^2), \varepsilon_6=\delta$	$2C_{66}\delta^2+O(\delta^4)$
	T3	$\varepsilon_1=\delta, \varepsilon_2=-\delta, \varepsilon_3=\delta^2/(1-\delta^2)$	$(C_{11}-C_{12})\delta^2+O(\delta^4)$
	T4	$\varepsilon_1=\delta, \varepsilon_2=\delta^2/(1-\delta^2), \varepsilon_3=-\delta$	$\frac{(C_{11}-2C_{13}+C_{33})}{2}\delta^2+O(\delta^4)$
	T5	$\varepsilon_1=\delta, \varepsilon_2=\delta, \varepsilon_3=\delta$	$(C_{11}+C_{12}+2C_{13}+C_{33}/2)\delta^2+O(\delta^4)$
	T6	$\varepsilon_3=\delta$	$\frac{C_{33}}{2}\delta^2$
Martensite 5M	O1	$\varepsilon_1=\delta$	$\frac{C_{11}}{2}\delta^2$
	O2	$\varepsilon_2=\delta$	$\frac{C_{22}}{2}\delta^2$
	O3	$\varepsilon_3=\delta$	$\frac{C_{33}}{2}\delta^2$
	O4	$\varepsilon_1=\delta^2/(1-\delta^2), \varepsilon_4=\delta$	$2C_{44}\delta^2+O(\delta^4)$
	O5	$\varepsilon_2=\delta^2/(1-\delta^2), \varepsilon_5=\delta$	$2C_{55}\delta^2+O(\delta^4)$
	O6	$\varepsilon_3=\delta^2/(1-\delta^2), \varepsilon_6=\delta$	$2C_{66}\delta^2+O(\delta^4)$
	O7	$\varepsilon_1=-\delta, \varepsilon_2=\delta^2/(1-\delta^2), \varepsilon_3=\delta$	$\frac{1}{2}(C_{11}-2C_{13}+C_{33})\delta^2+O(\delta^4)$
	O8	$\varepsilon_1=\delta, \varepsilon_2=-\delta, \varepsilon_3=\delta^2/(1-\delta^2)$	$\frac{1}{2}(C_{11}-2C_{12}+C_{22})\delta^2+O(\delta^4)$
	O9	$\varepsilon_1=\delta^2/(1-\delta^2), \varepsilon_2=-\delta, \varepsilon_3=\delta$	$\frac{1}{2}(C_{22}-2C_{23}+C_{33})\delta^2+O(\delta^4)$

premartensite and the NM martensite of Ni_2MnGa by using DFT and further including contributions from the fixed-spin moment magnons to reveal the complete phase sequence between the three structures as a function of temperature. The role of the vibrational and electronic contribution of the free energy to lattice instability has also been discussed by Chernenko et al. [17] from the results of the low-temperature specific heat measurement for Ni–Mn–Ga alloys.

Experimental studies show that martensitic transformation is characterized by the coupling of the soft phonon modes and pronounced softening of the shear modulus $C' = 1/2(C_{11} - C_{12})$ of the parent phase [8,18–20]. Inspired by these observations, Hu et al. [21] recently calculated the composition dependent elastic modulus for off-stoichiometric $L2_1$-Ni_2MnGa by investigating the correlation between elastic modulus and martensitic transition temperature or e/a ratio by constructing stable cite occupancy. Unfortunately, the behavior of elastic properties of martensite structure is still insufficient in the literature. In our previous study [22], we predicted the elastic constants for both cubic $L2_1$ and NM tetragonal martensitic structure of Ni_2MnGa using the potential with large number of valence electrons. However, the elastic modulus for 5M modulated tetragonal structure remains unknown.

We are particularly interested in the calculation of the elastic constants for Ni_2MnGa in this study, since the determination of elastic constants is essential in designing of almost all applications of MSMAs. The knowledge of full anisotropic elastic constants provide the basis of the *magneto-mechanical coupling*, in addition to supplying information on strength of the materials, mechanical stability, phase transitions, and the anisotropic character of the bonding. The elastic properties are also used to determine measurable physical and thermodynamical properties, e.g. – transverse and longitudinal – speeds of sound which in turn may be used to estimate the Debye temperature.

We have performed spin-polarized total energy calculations by the use of first-principles methods based on DFT with the aim of developing microscopic understanding of MSM behavior of Ni_2MnGa. This paper is devoted to the study of mechanical properties of Ni_2MnGa in both austenitic and martensitic structures. To the best of our knowledge, this work presents the elastic constans of Ni_2MnGa in the structure of 5M martensite for the first time. We have also re-calculated elastic constants for cubic and NM structures by using the potential with $e/a = 7.5$. The elastic constants are predicted by straining the cubic $L2_1$, 5M pseudo-tetragonal and NM tetragonal martensitic structures. Because of the special significance of the isotropic bulk modulus, shear modulus, Young's modulus and Poisson's ratio for technological applications, we have also calculated these quantities from the elastic constants. The Debye temperatures of Ni_2MnGa are estimated from the average sound velocity.

2. Computational method

Spin-polarized total energy calculations have been performed within the framework of the DFT by using the Vienna *ab initio* simulation package (VASP) program [23]. We have used the pseudopotential with $3p^6 3d^8 4s^2$ for Ni, $3p^6 3d^5 4s^2$ for Mn, and $3d^{10} 4s^2 4p^1$ for Ga as the valence configurations to calculate the structural parameters of cubic austenitic, NM and 5M martensitic phases, and also elastic constants of cubic austenitic and NM martensitic phases of stoichiometric Ni_2MnGa in our previous work [22]. The computational method for structural properties is given in detail in the same study [22] and will not be repeated here. We should note that, in this study the valence electronic configurations for Ni and Mn are changed to $3d^8 4s^2$ and $3d^5 4s^2$ respectively, while keeping Ga valence configuration as $3d^{10} 4s^2 4p^1$. This offers a shorter run time and utilizes less memory than hard-pseudopotential used in the previous study; it additionally enables efficient calculation of the elastic constants of modulated structures. We have checked the effect of the number of valence electrons on the structural parameters and elastic constants by repeating the calculations for only austenitic phase for two potentials, and we found at most 3% difference. Hence, we have taken the structural parameters obtained in our previous study [22] and calculated the elastic constants for three phases by using the specified valence configurations above. Note that the $e/a = 7.5$ value results from accounting the 3d electrons of Ga in the core rather than valence due to their small contribution of Ga 3d electrons to the cohesion.

There are two methods in calculating the elastic constants from first principles: one is related to the analysis of the calculated total energy of a crystal as a function of applied strain. The second one is based on the analysis of changes in the calculated stress values arising from variation in the strain. In our calculation, we choose the first method to predict the elastic constants. For the deformation of a crystal in a linear elastic manner at small strain, the energy of the strained system can be expressed by a Taylor series expansion as:

$$E(V,\varepsilon) = E(V_0,0) + V_0\sum_{i=1}^{6}\sigma_i\varepsilon_i + \frac{V_0}{2}\sum_{i,j=1}^{6}C_{ij}\varepsilon_i\varepsilon_j + O(\varepsilon^3), \quad (1)$$

where ε and σ are the strain and stress tensors, respectively. V_0 is the volume of the unstrained lattice, $E(V_0, 0)$ is the corresponding total energy, and C_{ij} are the elastic constants. The elastic constants are identified as proportional to the second order coefficient in a polynomial fit of the total energy as a function of the distortion parameter.

3. Results and discussion

The elastic constants for three phases of Ni_2MnGa considered in this work are calculated for the minimized crystal structure obtained from our previous study [22]. The three independent elastic constants for cubic phases, the six for NM martensitic phase, and the nine for 5M martensitic phase are determined by imposing three, six and nine different deformations, respectively, on the equilibrium strain free unit cell. The components of each strain tensor (a 6-vector in Voigt notation) and the corresponding expressions for the strain energy densities are given in Table 1. For each lattice structure of Ni_2MnGa studied, we strained the lattice by varying the strain parameter, δ, from −0.03 to 0.03 in steps of 0.01 to obtain the total minimum energies at these strains. Fig. 1a–c illustrates the total energy as a function of strain for the three distortions, the six distortions, and nine distortions for cubic, NM and 5M structures, respectively. The lines in the figures represent the third order polynomial fit to the energy versus strain curve. Then, the elastic constants are extracted from the second order coefficient of this fit.

A cubic crystal has three independent elastic moduli obtained from the bulk modulus $B=(C_{11}+2C_{12})/3$ and two shear moduli of $C_{11}–C_{12}$ and C_{44}. For the calculation of the bulk modulus, we consider cubic strain tensor of C1 shown in Table 1 with energy change $\Delta E=(3/2)V_0(C_{11}+C_{12})\delta^2$. The shear moduli of $C_{11}–C_{12}$ and C_{44} are obtained by applying orthorhombic (C2) and monoclinic (C3) volume conserving strains, respectively. The results for the bulk modulus, the elastic stiffness constants C_{ij}, and the elastic compliances S_{ij} of the austenitic phase are presented in Table 3. The components of S_{ij} are calculated from the C_{ij} using the following relations:

$$S_{44}=\frac{1}{C_{44}}, \tag{2}$$

$$S_{11}-S_{12}=\frac{1}{C_{11}-C_{12}}, \tag{3}$$

$$S_{11}+S_{12}=\frac{C_{11}}{(C_{11}-C_{12})(2C_{12}+C_{11})}. \tag{4}$$

They are in agreement with the experimental elastic constants of Ni_2MnGa in the $L2_1$ structure obtained by ultrasonic measurements determined between room temperature and the intermediate pre-martensitic phase transition temperature [18,24] and other theoretical calculations [21,25]. While the accuracy of the bulk modulus calculated for cubic phase, showing a deviation of 6.7% from the experiment performed by Worgull et al. [24] and 46% from the experiment carried out by Manosa et al. [18], is comparable to that of the other calculations [21,25]. Our value for C', tetragonal shear constant, found as 5.5 GPa, compares well with the experimental values for $L2_1$ structure obtained by ultrasonic measurements ranging between 4.5 GPa [24] and 22 GPa [18].

We applied the six strains listed in Table 1 in order to determine the elastic constants of martensitic NM tetragonal structure of Ni_2MnGa. The expression for corresponding strain energy densities are also given in the same table. The first four strains (T1–T4) in Table 1 are selected to be volume conserving to minimize the change in the basis set related with the applied strain. However, the last one yielding C_{33} is accompanied by a volume change, but preserves the symmetry of the $L2_1$ lattice. The strains T1, T2 and T6 give directly the C_{44}, C_{66}, C_{33}, respectively. The remaining elastic constants of C_{11}, C_{12}, and C_{13} are obtained from the energy expressions resulted from the distortion matrices of T3, T4, and T5. The T5 distortion induced by hydrostatic stress yields the expression for bulk modulus as $9B/2=C_{11}+C_{12}+2C_{13}+C_{33}/2$, resulting in $B=158$ GPa. The elastic constants of C_{11}, C_{12}, C_{13}, C_{33}, C_{44} and C_{66} are found as 252, 74, 144, 194, 100, and 55 GPa, respectively, as shown in Table 2. Listed also in the same table are the compliances S_{ij} for tetragonal

Table 2
The bulk modulus B (GPa), the elastic constants C_{ij} (GPa), and the corresponding elastic compliances S_{ij} (TPa^{-1}) of Ni_2MnGa alloy calculated in the cubic $L2_1$ and martensitic structures of NM and 5M, compared with available experiments and previous theoretical calculations.

Phase		B	C'	C_{11}	C_{12}	C_{13}	C_{22}	C_{23}	C_{33}	C_{44}	C_{55}	C_{66}	S_{11}	S_{12}	S_{13}	S_{22}	S_{23}	S_{33}	S_{44}	S_{55}	S_{66}
Austenite	Our cal.	155.7	5.5	163	152					107			61.3	−29.6					9.35		
	Exp. [24]	146.0	4.5	152	143					103											
	[18]	106.7	22	136	92					102											
	Other cal. [21]	152.1	15.9	173	141.3					99.4											
	[25]	149.7	2.5	153	148					100											
Martensite NM	Our cal.	158.0	89	252	74	144			194	100		55	7.26	1.65	−6.61			15.0	10.0		18.2
Martensite 5M	Our cal.	153.2	107	271	56	135	265	127	194	91	100	15	5.84	1.04	−4.74	5.68	−4.44	11.4	11.0	10.0	66.7

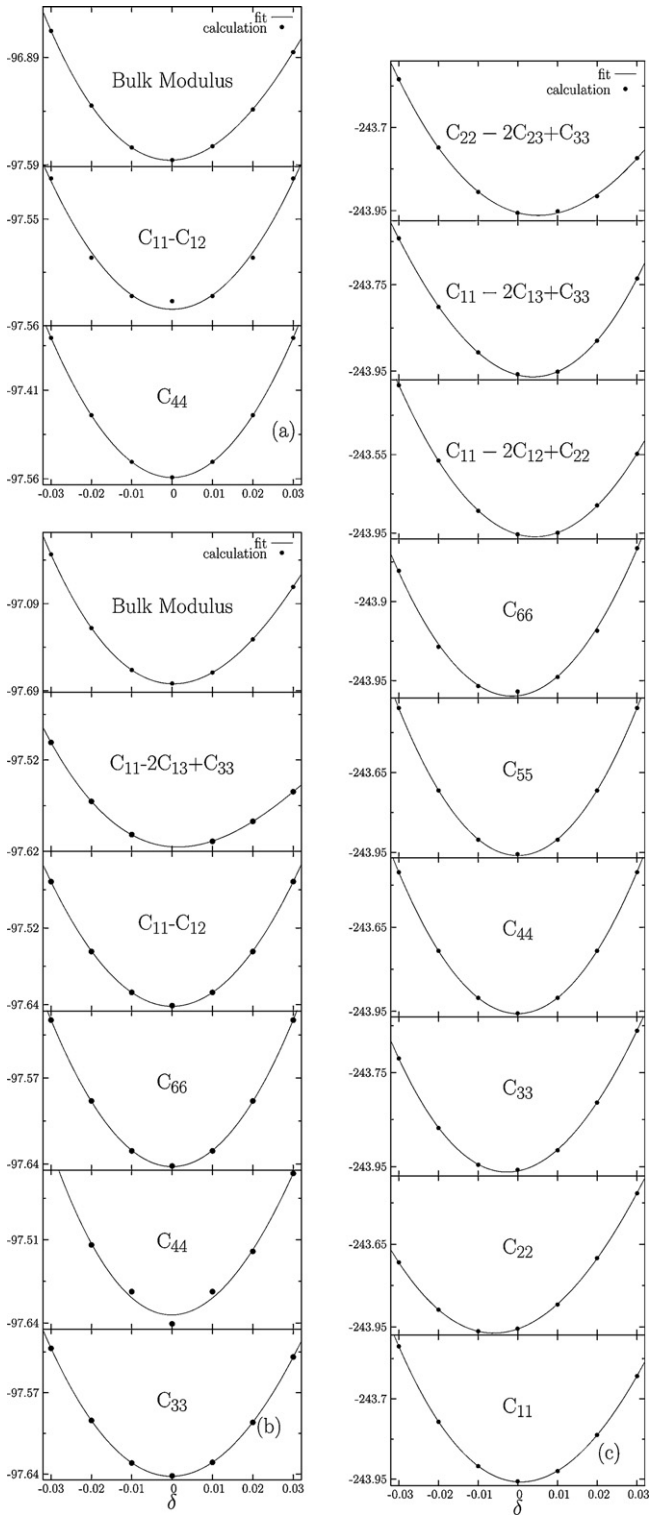

Fig. 1. Total energy as a function of strain (δ) for Ni_2MnGa in the structures of (a) cubic $L2_1$, (b) tetragonal NM martensite, and (c) 5M martensite. The circles represent the calculated values, the solid line is the polynomial fit.

structure obtained from the following relations:

$$S_{11} + S_{12} = \frac{C_{33}}{C}, \tag{5}$$

$$S_{11} - S_{12} = \frac{1}{C_{11} - C_{12}}, \tag{6}$$

$$S_{13} = -\frac{C_{13}}{C}, \tag{7}$$

$$S_{33} = \frac{C_{11} + C_{12}}{C}, \tag{8}$$

$$S_{44} = \frac{1}{C_{44}}, \tag{9}$$

$$S_{66} = \frac{1}{C_{66}}, \tag{10}$$

where $C = (C_{11} + C_{12})C_{33} - 2C_{13}^2$.

In Table 2, we also present the elastic constants of martensitic 5M modulated structure of $L2_1$. The stability of this structure is achieved from the orthorhombic supercell of 40 atoms formed by five tetragonal crystallographic unit cells. Hence, we need nine different strains to determine nine independent elastic constants. The distortions used for 5M modulated structures and the corresponding strain energy densities are described in the last row of Table 1. The first three elastic constants of C_{11}, C_{22}, and C_{33} are obtained by means of deformations (O1, O2, O3) of the lattice involving the orthorhombic symmetry. The three different volume conserving monoclinic shear distortions of O4, O5, and O6 are employed in determining the shear elastic constants of C_{44}, C_{55}, and C_{66}, respectively. The remaining elastic constants of C_{12}, C_{13}, and C_{23} are calculated from a combination of three volume conserving orthorhombic deformations (O7, O8, and O9). Table 2 also displays the results for the elastic stiffness constants, as well as the compliances of orthorhombic structure. The relations between the stiffness and compliance constants for the orthorhombic phase are given as:

$$S_{11} = \frac{C_{23}{}^2 - C_{22}C_{33}}{C} \tag{11}$$

$$S_{12} = \frac{C_{12}C_{33} - C_{13}C_{23}}{C} \tag{12}$$

$$S_{13} = \frac{C_{13}C_{22} - C_{12}C_{23}}{C}, \tag{13}$$

$$S_{22} = \frac{C_{13}{}^2 - C_{11}C_{33}}{C}, \tag{14}$$

$$S_{23} = \frac{C_{11}C_{23} - C_{12}C_{13}}{C}, \tag{15}$$

$$S_{33} = \frac{C_{12}{}^2 - C_{11}C_{22}}{C}, \tag{16}$$

$$S_{44} = \frac{1}{C_{44}}, \tag{17}$$

$$S_{55} = \frac{1}{C_{55}}, \tag{18}$$

$$S_{66} = \frac{1}{C_{66}}, \tag{19}$$

where $C = C_{13}{}^2C_{22} - 2C_{12}C_{13}C_{23} + C_{11}C_{23}{}^2 + C_{12}{}^2C_{33} - C_{11}C_{22}C_{33}$.

There are not any measurements or any other theoretical studies for all of the elastic constants for both NM and 5M martensitic structures of Ni_2MnGa alloy to compare with our results. The elastic stiffness coefficients for both austenitic and martensitic phases shown in Table 2 obey the generalized elastic stability criteria [26] for cubic, tetragonal and orthorhombic crystals. This indicates that $L2_1$, 5M and NM structures are mechanically stable. Moreover, these stability conditions lead to some restrictions on the magni-

tude of bulk modulus. They can be written as:

$$\begin{aligned} C_{12} < B_o < C_{11}, \\ \frac{1}{3}(C_{12}+2C_{13}) < B_o < \frac{1}{3}(C_{11}+2C_{33}), \\ \frac{1}{3}(C_{12}+C_{13}+C_{23}) < B_o < \frac{1}{3}(C_{11}+C_{22}+C_{33}) \end{aligned} \quad (20)$$

for cubic, tetragonal and orthorhombic structures, respectively. The bulk modulus found as 155.7, 158.0 and 153.2 GPa for austenitic, NM and 5M martensitic structures satisfies the restrictions given in Eq. (20). We obtain a significantly low value for the tetragonal shear constant C' of the parent phase. This is 16 and 19 times smaller than the values obtain for NM and 5M martensitic phases. This small value is significant in understanding the observed large deformation upon transition. Calculations indicate that only a small decrease in the *shear elastic* constant cause phase transition. The ratio of two shear constants C_{44}/C' can be used as an elastic anisotropy factor for cubic crystals. We calculate it as 17.6, which is in good agreement with the values of the experiments ranging between 5 and 23 [18,24]. This important high value of the elastic anisotropy is resulted from the remarkable softening of C' at the phase transition.

Earlier studies show that the first martensite transition on cooling depends on the composition, and $L2_1$ structure favors phase transition into the martensite in the order of 5M, 7M and NM structures upon cooling [4,14,27]. According to X-ray diffraction data [11], only the NM phase exist for $e/a > 7.71$ and $T_M > 353$ K while layered phases (5M and 7M) are observed at lower values of e/a and T_M. In this sense, T_M and e/a of NM structure are larger than those of 7M and 5M structures. As seen from Table 2, when the phase transformation from austenite to martensite occurs, tetragonal shear constant C' drastically increases, but C_{44} monotonically decreases. While the martensitic transformation from 5M to NM (through 7M) in which e/a and T_M rise takes place, the C' decreases, but C_{44} increases. This is confirmed by the previous study in which the elastic constants were calculated for different kinds of off-stoichiometric $L2_1$-Ni_2MnGa [21]. The values for the bulk modulus show little variation with respect to structures.

The elastic constants shown in Table 2 are for the Ni_2MnGa single crystals. In the applications, single crystal properties do not show the mechanical properties at the larger scale. Moreover, when the single crystal samples are not produced experimentally, polycrystalline samples are used to determine the elastic moduli. Hence, the individual elastic constants C_{ij} cannot be measured. Instead, bulk modulus B and shear modulus G are obtained. Hence, we consider the calculation of polycrystalline aggregates of Ni_2MnGa from the theoretical single crystal properties. There are two approximation methods to derive the isotropic elastic moduli for polycrystalline single-phase materials by averaging the anisotropic single crystal elastic properties over all possible orientations of crystallites. They are the Voigt and Reuss methods representing the upper and lower bounds, respectively, to the isotropic elastic modulus [28–30]. According to the Voigt approximation, assuming uniform strain through the sample the shear modulus (G_V) in the cubic system is given by the following equations:

$$G_V = \frac{C_{11}-C_{12}+3C_{44}}{5}. \quad (21)$$

Averaging according to Reuss method assuming uniform stress in the polycrystalline aggregate leads to

$$G_R = \frac{5}{4(S_{11}-S_{12})+3S_{44}}. \quad (22)$$

The bulk modulus B is the same in both the Voigt and Reuss averages in the cubic system and it is given by the following equation:

$$B = B_V = B_R = \frac{C_{11}+2C_{12}}{3}. \quad (23)$$

Hill [31] has discovered that the arithmetic average of the Voigt and the Reuss bounds, called as Voigt–Reuss–Hill (VRH) average, represents the best estimation of the isotropic elastic moduli. Using VRH average, the shear and bulk modulus are taken as $G = 1/2(G_V + G_R)$ and $B = 1/2(B_V + B_R)$, respectively.

For the tetragonal NM phase of Ni_2MnGa, the isotropic averaged shear modulus is bounded from above by the Voigt approximation:

$$B_V = \frac{1}{9}(2C_{11}+2C_{12}+4C_{13}+C_{33}) \quad (24)$$

and from below by the Reuss approximation;

$$B_R = \frac{1}{2(S_{11}+S_{12})+S_{33}+4S_{13}}. \quad (25)$$

Correspondingly, the Voigt and Reuss shear modulus of polycrystalline NM tetragonal phase are given by:

$$G_V = \frac{1}{15}(2C_{11}-C_{12}-2C_{13}+C_{33}+6C_{44}+3C_{66}) \quad (26)$$

and

$$G_R = \frac{15}{(8S_{11}-4S_{12}-8S_{13}+4S_{33}+6S_{44}+3S_{66})}, \quad (27)$$

respectively.

Analogous expressions hold for the orthorhombic structure of 5M modulation. Bulk modulus is bounded from above by:

$$B_V = \frac{1}{9}(C_{11}+C_{12}+C_{33}+2(C_{12}+C_{13}+C_{23})), \quad (28)$$

and below by

$$B_R = \frac{1}{S_{11}+S_{22}+S_{33}+2(S_{12}+S_{13}+S_{23})}. \quad (29)$$

The Voigt shear modulus and Reuss shear modulus are defined as:

$$\begin{aligned} G_V = \frac{1}{15}(C_{11}+C_{22}+C_{33}-C_{12}-C_{13} \\ -C_{23}+3C_{44}+3C_{55}+3C_{66}), \end{aligned} \quad (30)$$

and

$$G_R = \frac{15}{4(S_{11}+S_{22}+S_{33})-4(S_{12}+S_{13}+S_{23})+3(S_{44}+S_{55}+S_{66})}, \quad (31)$$

respectively.

From the results of the elastic stiffness (C_{ij}) and compliance constants (S_{ij}) given in Table 2, the elastic moduli of polycrystalline Ni_2MnGa in the three structures of interest in this study are determined by using the Voigt–Reuss–Hill averaging scheme given by the Eqs. (21)–(31). The results are listed in Table 3. The values of Voigt and Reuss bulk modulus calculated are nearly the same. However, the difference between two values of shear modulus is rather large, so we quote as one-half of the difference between the bounds. From Tables 2 and 3, we can see that the isotropic bulk modulus calculated from the elastic constants for the orthorhombic structure (Table 3) has nearly the same value as the single crystal bulk modulus obtained from applying hydrostatic pressure to the crystal (Table 2). As expected, because the elastic constants of cubic and tetragonal phases are obtained by using distortion matrix giving the expression for the bulk modulus, we get the same values of bulk modulus for two methods (Tables 2 and 3). The ratio of bulk to shear modulus of polycrystalline phases (B/G) proposed by Pugh [32] provides the information about the ductility of the material. A high (B/G) value is associated with the better ductility, while

Table 3
The isotropic bulk modulus B (GPa) and shear modulus G (GPa) for polycrystalline Ni_2MnGa from the single crystal elastic constants using Voigt, Reuss and Hill's approximations. The Young's modulus E (GPa) and the Poisson's ratio υ are predicted from Hill's approximation, along with the available experiments.

Phase	B_V	B_R	B	G_V	G_R	G	B/G	E	υ
Austenite	155.6	155.7	155.7	66.4	12.8	39.6 ± 26.8	3.93	109 107.9[c]	0.383 0.3[a,b] 0.38[c]
Martensite NM	158.0	157.8	157.9	73.8	53.8	63.6 ± 10.0	2.48	168	0.322
Martensite 5M	151.8	151.7	151.8	68.7	38.7	53.7 ± 15.0	2.82	144	0.342

[a] Taken from [33].
[b] Taken from [34].
[c] Taken from [35].

a low value represents more brittleness. The critical value differentiating the ductile material from the brittle material is about 1.75. Estimated from our calculations, the value of B/G is 3.93, 2.48 and 2.82 for cubic, tetragonal and orthorhombic structures of Ni_2MnGa, respectively. Therefore, Ni_2MnGa material can be classified as ductile material. However, these values are insufficient for the applications of MSM technology requiring more ductile material. We also obtained the Young's modulus E and Poisson ratio υ which are the parameters concerned with the shear strength and the hardness of the material. They are related to B and G by the following equations:

$$E = \frac{9BG}{3B + G} \tag{32}$$

and

$$\upsilon = \frac{3B - E}{6B}. \tag{33}$$

Listed also in Table 3 are the results for Young's modulus and Poisson's ratio of Ni_2MnGa in three structures. Poisson's ratio measures the stability of a crystal against shear strain, while Young's modulus measures the stiffness of an isotropic elastic material to linear strain. The higher value of Young's modulus calculated for martensitic structures indicates that the ferromagnetic Ni_2MnGa in the austenitic phase is less hardness material than in the martensitic structure. On the other hand, the Poisson ratio decreases, as expected, when this stoichiometric material goes into phase transition from austenite to martensite. The results of Young's modulus and Poisson's ratio calculated for cubic Ni_2MnGa are in good agreement with the experimental results (see Table 3) [33–35].

After we have calculated elastic constants of austenitic and martensitic structures, we are also interested in the variations of Debye temperature with respect to structure. Debye temperature is an important physical property when concerning elastic constants, specific heat and melting temperature. At low temperature, due to only the contribution of acoustic vibrational modes, the Debye temperature predicted from elastic constants is consistent with that determined from specific heat measurements. For low temperatures, we have estimated the Debye temperatures (θ_D) of Ni_2MnGa structures from the averaged sound velocity, v_m, by using the following relation [36]:

$$\theta_D = \frac{h}{k}\left[\frac{3n}{4\pi}\left(\frac{N_A\rho}{M}\right)\right]^{1/3} v_m, \tag{34}$$

where h is the Plank's constant, k is the Boltzman's constant, N_A is the Avogadro's number, ρ is the density, M is the molecular weight and n is the number of atoms in the molecules. The averaged sound velocity v_m is approximately predicted by the following equation [37]:

$$v_m = \left[\frac{1}{3}\left(\frac{2}{v_t{}^3} + \frac{1}{v_l{}^3}\right)\right]^{-1/3}, \tag{35}$$

Table 4
The longitudinal v_L (m/s), transverse v_T (m/s) and average sound velocity v_M (m/s) calculated from polycrystalline elastic modulus and Debye temperature θ_D (K) obtained from average sound velocity for Ni_2MnGa alloy in the austenitic and martensitic structures, along with the available experiments.

	v_L	v_T	v_M	θ_D
Austenite	5165	2251	2542	323 261[a]
Martensite NM	5572	2853	3196	406 345[a]
Martensite 5M	5346	2622	2944	374 278[a] 319[a]

[a] Taken from [17].

where v_l and v_t are the longitudinal and transverse elastic wave velocities of the isotropic material given by the following equations [38]:

$$v_l = \left(\frac{3B + 4G}{3\rho}\right)^{1/2} \quad \text{and} \quad v_t = \left[\frac{G}{\rho}\right]^{1/2}, \tag{36}$$

respectively. Here B and G are the polycrystalline bulk modulus and shear modulus, respectively.

The wave velocities and Debye temperatures calculated for Ni_2MnGa in the austenitic and martensitic structures are given in Table 4. As seen from the table, Debye temperature for austenitic phase is smaller than that for martensitic phase, as confirmed by the experiments which show that specific heat C_P for austenite is larger than for martensite [38,39]. Moreover, an increase of Debye temperature is shown when the 5M–NM transformation happens. This behavior is in agreement with the low temperature specific heat measurements [17]. The values for Debye temperatures deviate from the experimental values [17] at most 23%.

4. Conclusion

The variation of anisotropic elastic constants upon phase transformations of Ni_2MnGa is investigated by first-principles DFT method. The main results can be given as the following:

- The single crystal elastic and the corresponding compliance constants are predicted by straining the cubic $L2_1$ austenitic, tetragonal NM and 5M modulated martensitic structures. The results for the elastic constants of parent phase are in good agreement with those of available experiments and other theoretical calculations. Those for 5M martensitic structure are calculated for the first time in this study. Our results for elastic constants, which obey the stability conditions, show that the austenitic and martensitic structures are mechanically stable against the deformations applied.
- Considerably small value for the tetragonal shear constant, C' of austenitic phase indicates the ease of the phase transition

into martensitic phase. The tetragonal shear constant C' sharply increases when the phase transition from austenite to martensite occurs. On the other hand, C' decreases as 5M transform to NM phase (through 7M structure). In contrast, the pure shear constant C_{44} shows an increase upon phase transitions. The pure shear constant, C_{66}, for 5M martensite is 15 GPa, though larger compared to austenite C' (5.5 GPa) value, still smaller than the C_{66} value (55 GPa) for NM martensite. This may thermodynamically drive the transformation to final NM martensite through 7M martensitic phase. The calculated values of Young's modulus and Poisson's ratio indicate that the martensitic structure is harder than the austenitic structure.

- The Debye temperatures for Ni_2MnGa in the different structures are obtained by using the average sound velocity. The trend of Debye temperature as a function of e/a (phase transformation from austenite to 5M and 5M to NM) is consistent with the behavior of the experiment.

In summary, we have computed the mechanical properties of Ni_2MnGa in the cubic, NM and 5M structures relevant for its technological applications. The results for 7M modulation are not given in this work due to large computational requirements. In the future, the structural, mechanical and electronic properties of 7M phase will be investigated.

Acknowledgements

Authors would like to thank the following institutions and agencies in carrying out this work. Computations are carried out on TUBITAK-ULAKBIM clusters. The authors acknowledge the support by NSF-IMI IIMEC for the research presented in this paper. Dr. Cagin would also like to acknowledge the support of TUBITAK for BIDEP facilitating the visits to Turkey to complete the study.

References

[1] S.J. Murray, M. Marioni, S.M. Allen, R.C. O'Handley, T.A. Lograsso, Appl. Phys. Lett. 77 (6) (2000) 886–888.
[2] I. Aaltio, K. Ullakko, Proceedings of the 7th International Conference on New Actuators ACTUATOR 2000, Bremen, Germany, 2000, p. 45.
[3] A. Sozinov, A.A. Likhachev, N. Lanska, K. Ullakko, Appl. Phys. Lett. 80 (2002) 1746–1748.
[4] V. Mortynov, V. Kokorin, J. Phys. III (France) 2 (1992) 739–750.
[5] S.J. Murray, M. Marioni, S.M. Allen, R.C. O'Handley, T.A. Lograsso, Appl. Phys. Lett. 77 (2000) 886–888.
[6] O. Heczko, A. Sozinov, K. Ullakko, IEEE Trans. Magn. 36 (5) (2000) 3266–3268.
[7] A. Sozinov, A.A. Likhachev, N. Lanska, O. Söderberg, K. Koho, K. Ulakko, V.K. Lindroos, J. Phys. IV 115 (2004) 121–128.
[8] V.A. Chernenko, J. Pons, C. Segui, E. Cesari, Acta Mater. 50 (2002) 53–60.
[9] P. Entel, V.D. Buchelnikov, V.V. Khovailo, A.T. Zayak, W.A. Adeagho, M.E. Gruner, H.C. Herpor, E.F. Wassermann, J. Phys. D: Appl. Phys. 39 (2006) 865–889.
[10] V. Chernenko, V. L'vov, E. Cesari, J. Pons, R. Portier, S. Zagorodnyuk, Mater. Trans. JIM 43 (2002) 856–860.
[11] N. Lanska, O. Söderberg, A. Soziniv, Y. Ge, K. Ullakko, V.K. Lindroos, J. Appl. Phys. 95 (2004) 8074–8078.
[12] V.A. Chernenko, Scripta Mater. 40 (1999) 523–527.
[13] K. Tsuchiya, H. Nakamura, D. Ohtoyo, H. Nakayama, M. Umemoto, H. Ohtsuka, J. Phys. IV France 11 (Pr8) (2001) 263–268.
[14] J. Pons, V.A. Chernenko, R. Santamarta, E. Cesari, Acta Mater. 48 (2000) 3027–3038.
[15] J. Enkovaara, A. Ayuela, L. Nordström, R.M. Nieminen, J. Appl. Phys. 91 (2002) 7798–7800.
[16] M.A. Uijttewaal, T. Hickel, J. Neugebauer, M.E. Gruner, P. Entel, Phys. Rev. Lett. 102 (2009) 035702.
[17] V.A. Chernenko, A. Fujita, S. Besseghini, J.I. Perez-Landazabal, J. Magn. Magn. Mater. 320 (2008) e156–e159.
[18] L. Manosa, A. Gonzalez-Comas, E. Obrado, A. Planes, Phys. Rev. B 55 (1997) 11068–11071.
[19] M. Stipcich, L. Manosa, A. Planes, M. Morin, J. Zarestky, T. Lograsso, C. Stassis, Phys. Rev. B 70 (2004) 054115.
[20] P.J. Brown, J. Crangle, T. Kanomata, M. Matsumota, K.-U. Neumann, B. Ouladdiaf, K.R.A. Ziebeck, J. Phys.: Condens. Matter. 14 (2002) 10159–10171.
[21] Q.M. Hu, C.M. Li, R. Yang, S.E. Kulkova, D.I. Bazhanov, B. Johansson, L. Vitos, Phys. Rev. B 79 (2009) 144112.
[22] S. Ozdemir Kart, M. Uludogan, I. Karaman, T. Cagin, Phys. Stat. Sol. (A) 205 (5) (2008) 1026–1035.
[23] G. Kresse, J. Furthmüller, Phys. Rev. B 54 (1996) 11169–11186;
G. Kresse, D. Joubert, Phys. Rev. B 59 (1999) 1758–1775.
[24] J. Worgull, E. Petti, J. Trivisonno, Phys. Rev. B 54 (1996) 15695–15699.
[25] C. Bungaro, K.M. Rqbe, A. Dal Corso, Phys. Rev. B 68 (2003) 134104.
[26] D.C. Wallace, Thermodynamics of Crystals, Wiley, New York, 1972.
[27] J. Enkovaara, A. Ayuela, A.T. Zayak, P. Entel, L. Nordströn, M. Dube, J. Jalkanen, J. Impola, R.M. Nieminen, Mater. Sci. Eng. A 378 (2004) 52–60.
[28] W. Voigt, Lehrbush der Kristallphysik, B.G. Taubner, Leipzig, 1928.
[29] A. Reuss, Z. Angew, Math. Mech. 9 (1929) 49–58.
[30] M. Bilge, H.H. Kart, S. Ozdemir Kart, T. Cagin, Mater. Chem. Phys. 111 (2008) 559–564.
[31] R. Hill, Proc. Phys. Soc. A 65 (1952) 349–354.
[32] S.F. Pugh, Phil. Mag. 45 (1954) 823–843.
[33] E. du Tremolet de Lacheisserie, J.C. Peuzin, J. Magn. Mater. 136 (1994) 189–196.
[34] M. Kohl, A. Agarwal, V.A. Chernenko, M. Ohtsuka, K. Seemann, Mater. Sci. Eng. A 438–440 (2006) 940–943.
[35] Z. Wang, M. Matsumoto, T. Abe, K. Oikawa, J. Qiu, T. Takagi, J. Tani, Mater. Sci. Forum 327–328 (2000) 489–492.
[36] O.L. Anderson, J. Phys. Chem. Solids 24 (1963) 909–917.
[37] E. Schreiber, O.L. Anderson, N. Soga, Elastic Constants and Their Measurements, McGraw-Hill, New York, 1973.
[38] M. Kreissl, K.–U. Neumann, T. Stephans, K.R.A. Ziebeck, J. Phys.: Condens. Matter 15 (2003) 3831–3839.
[39] E. Cesari, V.A. Chernenko, J. Font, J. Muntasell, Thermochim. Acta 433 (2005) 153–156.